Chapter 5
Power System Transient Stability Preventive and Emergency Control

Daniel Ruiz-Vega, Louis Wehenkel, Damien Ernst, Alejandro Pizano-Martínez and Claudio R. Fuerte-Esquivel

Abstract A general approach to real-time transient stability control is described, yielding various complementary techniques: pure preventive, open-loop emergency, and closed-loop emergency controls. Recent progress in terms of a global transient stability-constrained optimal power flow is presented, yielding in a scalable non-linear programming formulation which allows to take near-optimal decisions for preventive control with a computing budget corresponding only to a few runs of standard optimal power flow and time-domain simulations. These complementary techniques meet the stringent conditions imposed by the real-life applications.

5.1 Introduction[1]

Power system security is more and more in conflict with economic and environmental requirements. Security control aims at making decisions in different time horizons so as to prevent the system from being in undesired situations, and in particular to avoid large catastrophic outages. Traditionally, security control has been divided into two main categories: preventive and emergency control.

[1] Portions of this chapter have been reprinted, with permission, from L. Wehenkel and M. Pavella 2004, Preventive vs. emergency control of power systems, presented at the *Real-Time Stability Challenge Panel Session, Power Systems Conference and Exposition 2004,* New York, New York, 10–13 October 2004. © 2004 IEEE.

D. Ruiz-Vega (✉)
Instituto Politécnico Nacional, Mexico City, Mexico
e-mail: drv_liege@yahoo.com

L. Wehenkel · D. Ernst
University of Liège, Liège, Belgium

A. Pizano-Martínez
Universidad de Guanajuato, Salamanca, Mexico

C. R. Fuerte-Esquivel
Universidad Michoacana de San Nicolás de Hidalgo, Morelia, Mexico

S. C. Savulescu (ed.), *Real-Time Stability in Power Systems,*
Power Electronics and Power Systems, DOI 10.1007/978-3-319-06680-6_5,

In preventive security control, the objective is to prepare the system when it is still in normal operation, so as to make it able to face future (uncertain) events in a satisfactory way. In emergency control, the disturbing events have already occurred, and thus the objective becomes to control the dynamics of the system in such a way that consequences are minimized.

Preventive and emergency controls differ in many respects, among which we list the following (Wehenkel 1999).

Types of Control Actions Generation rescheduling, network switching reactive compensation, sometimes load curtailment for preventive control; and direct or indirect load shedding, generation shedding, shunt capacitor or reactor switching, and network splitting for emergency control.

Uncertainty In preventive control, the state of the system is well known but disturbances are uncertain; in emergency control, the disturbance is certain, but the state of the system is often only partially known; in both cases, dynamic behavior is uncertain.

Open Versus Closed Loop Preventive control is generally of the open-loop feedforward type; emergency control may be closed loop, and hence more robust with respect to uncertainties.

In the past, many utilities have relied on preventive control in order to maintain system security at an acceptable level. In other words, while there are many emergency control schemes installed in reality, the objective has been to prevent these schemes as much as possible from operating, by imposing rather high objectives to preventive security control.

As to any rule, there are exceptions: for example, controlled generation shedding has been used extensively in Northern America to handle transient stability problems; in the same way, corrective control has been used in many systems as an alternative to preventive control in the context of thermal overload mitigation.

Nowadays, where the pressure is to increase trading and competition in the power system field, preventive security control is being considered as an impediment to competition; in turn, this breeds strong incentives to resort less on preventive control and more often on emergency control.

The objective of this chapter is essentially twofold: first, to concentrate on transient stability control, both preventive and emergency, and describe a general methodology able to realize convenient tradeoffs between these two aspects; second, to suggest means of integrated security control, coordinating various types of security (steady-state, voltage, and transient stability).

The general methodology used to design transient stability control techniques relies on the transient stability method called Single-Machine Equivalent (SIME). In what follows, we first describe the fundamentals of SIME and then concentrate on the advocated control techniques.

5.2 A Unified Approach to Transient Stability Assessment and Control

5.2.1 Fundamentals of SIME

SIME is a hybrid direct-temporal transient stability method (Pavella et al. 2000a).

Basically, SIME replaces the dynamics of the multi-machine power system by that of a suitable One-Machine Infinite Bus (OMIB) system. By refreshing continuously the OMIB parameters and by assessing the OMIB stability via the Equal-Area Criterion (EAC), SIME provides an as accurate Transient Stability Assessment (TSA) as the one provided by the multi-machine temporal information and, in addition, stability margins and critical machines.

In other words, SIME preserves the advantages of the temporal description (flexibility with respect to power system modeling, accuracy of TSA, and handling of any type of instability (first or multi-swing, plant, or inter-area mode)), and, in addition, complements them with functionalities of paramount importance.

One of them is generation control (generation rescheduling for preventive control, generation shedding for emergency control), which uses the knowledge of stability margins and critical machines. Indeed, the amount of generation to shift (or shed) depends on the size of the stability margin, and the generators from which to shift (or shed) are the so-called critical machines.

SIME-based preventive control relies on the temporal information (swing curves) provided by a Time-Domain (T-D) simulation program, whereas SIME-based emergency control relies on real-time measurements. Nevertheless, conceptually, the core of the method is the same. In what follows we assume that SIME is fed sequentially by samples of the multi-machine swing curves, no matter whether they are provided by T-D simulations or real-time measurements.

5.2.2 Instability Conditions and Margins

To analyze an unstable case (defined by the pre-fault system operating conditions and the contingency scenario), SIME starts receiving samples of the swing curves as soon as the system enters its post-fault configuration.

At each new sample, SIME transforms the multi-machine swing curve sample into a suitable OMIB equivalent, defined by its angle δ, speed ω, mechanical power P_{m}, electrical power P_{e}, and inertia coefficient M. All OMIB parameters are derived from multi-machine system parameters; Pavella et al. 2000a. Further, SIME explores the OMIB dynamics by using the EAC. The procedure stops as soon as the OMIB reaches the EAC *instability conditions* expressed by

$$P_{\mathrm{a}}(t_u) = 0 \text{ and } \dot{P}_{\mathrm{a}}(t_u) > 0, \tag{5.1}$$

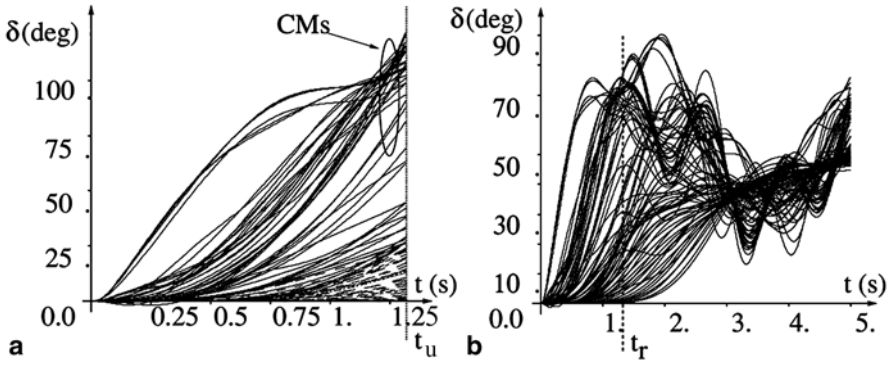

Fig. 5.1 Multi-machine swing curves. **a** Unstable case. **b** Stable case. Critical clearing time, 69 ms; clearing time, 95 ms. (Adapted from Ruiz-Vega 2002)

where P_a is the OMIB accelerating power, difference between P_m and P_e, and t_u is the *time to instability*: At this time, the OMIB system loses synchronism, and the system machines split irrevocably into two groups: the group of "advanced machines" that we will henceforth refer to as the "*Critical Machines*" (CMs), and the remaining ones, called the "*Non- critical Machines,*" (NMs)[2]. Thus, at t_u SIME determines:

- The CMs, responsible of the system loss of synchronism;
- The corresponding unstable margin:

$$\eta_u = A_{dec} - A_{acc} = -\frac{1}{2} M \omega_u^2. \tag{5.2}$$

Figures 5.1a to 5.3b illustrate the above definitions on a stability case simulated on the EPRI 88-machine system. More precisely, Fig. 5.1a, b portrays the multi-machine swing curves provided by a T-D program, stopped at "the time to instability", t_u. The symbol P_C used in the captions denotes the total power of the group of critical machines.

Figure 5.2a, b depicts the equivalent OMIB swing curve, whereas Fig. 5.3a, b represents, in the δ–P plane, the evolution with δ of the OMIB powers P_m and P_e.

[2] The "advanced machines" are the CMs for upswing instability phenomena, while for backswing phenomena they become NMs.

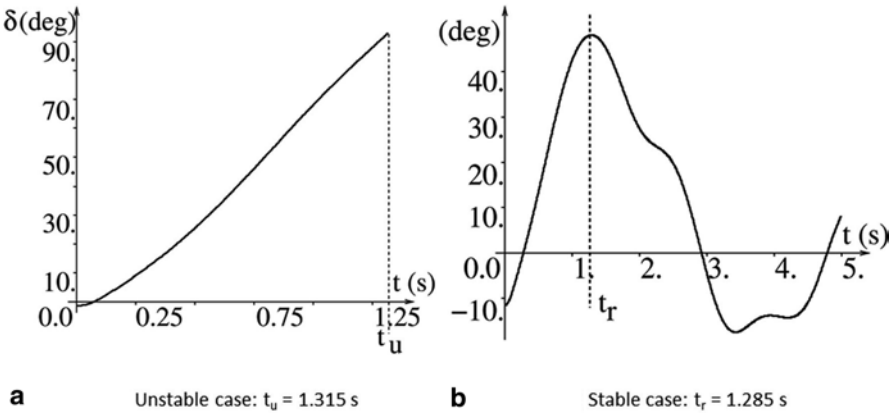

Fig. 5.2 Corresponding OMIB swing curves. **a** Unstable case. **b** Stable case. (Adapted from Ruiz-Vega 2002)

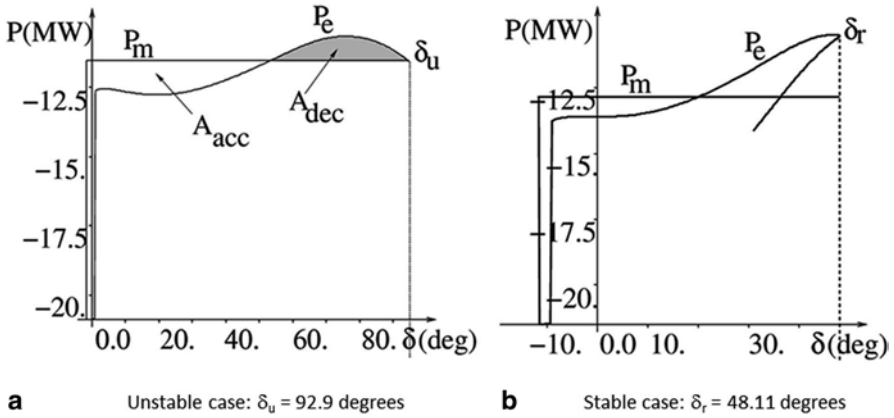

Fig. 5.3 Corresponding OMIB δ–P curves. **a** Unstable case. **b** Stable case. (Adapted from Ruiz-Vega 2002)

5.2.3 Salient Parameters and Properties

1. Calculation of stability margins, identification of the critical machines, and assessment of their degree of criticality (or participation to the instability phenomena) are parameters of paramount importance.
2. The "time to instability," t_u, is another important factor. It indicates the speed of loss of synchronism and measures its severity.
3. Under very unstable conditions, it may happen that the standard margin does not exist, because the OMIB P_m and P_e curves do not intersect (there is no post-

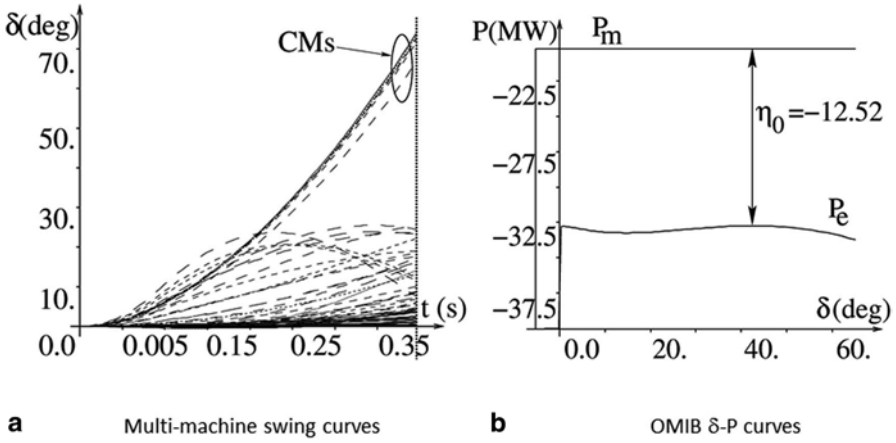

Fig. 5.4 Example of a severely stressed case. **a** Multi-machine swing curves. **b** OMIB *δ–P curves*. Clearing time = 95 ms; P_c = 5600 MW. (Adapted from Ruiz-Vega 2002)

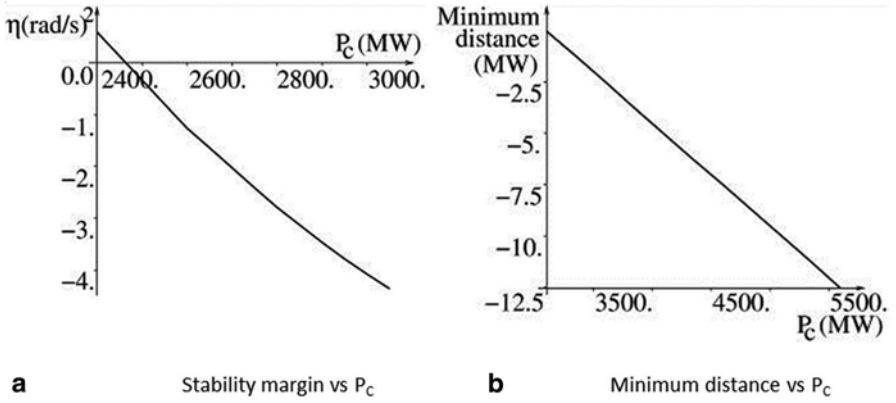

Fig. 5.5 Typical variations of the standard stability margin and of its surrogate with PC. **a** Stability margins versus P_c. **b** Minimum distance versus P_c. (Adapted from Ruiz-Vega 2002)

fault equilibrium solution). A convenient substitute is the "minimum distance" between post-fault P_m and P_e curves. Figure 5.4 illustrates this surrogate margin under particularly stressed conditions Ruiz-Vega and Pavella 2003. Note that here the surrogate to the "time to instability" is the time to reach this minimum distance and to stop the simulation. To simplify, we will still denote it "t_u".

4. A very interesting general property of the instability margins (standard as well as surrogate ones) is that they often vary quasi-linearly with the stability conditions (Pavella et al. 2000a). Figure 5.5 illustrates the margin variation with the total generation power of the group of critical machines, P_C. The proposed control techniques benefit considerably from this property.

5. On stability conditions and margins. Similar to the instability conditions (5.1), stability conditions are defined by (Pavella et al. 2000a)

$$\omega(t_r) = 0 \text{ and } P_a(t_r) < 0, \tag{5.3}$$

where time t_r denotes the *time to stability:* At this time, the OMIB angle reaches its maximum excursion, after which it starts decreasing. At t_r, the first-swing stable margin can be computed by (Pavella et al. 2000a)

$$\eta_{st} = \int_{\delta_r}^{\delta_u} P_a \, d\delta. \tag{5.4}$$

Figures 5.1*b* and 5.2*b* portray, respectively, the multi-machine swing curves provided by an Extended Transient Midterm Stability Program (ETMSP) T-D simulation stopped at the maximum integration period (5 s) and the corresponding OMIB swing curves. Figure 5.3b represents, in the δ–P plane, the evolution with δ of powers P_{m} and P_{e}; to simplify, only part of the evolution of the electrical power P_{e} has been displayed. Three observations should be made about stability conditions and margins. First, strictly speaking, stable cases do not have an OMIB equivalent (the system does not lose synchronism and its machines do not split into two divergent groups). However, by continuation, one can still use the OMIB corresponding to an unstable case close enough to the stable one. Second, meeting the stability conditions (5.3) does not guarantee that the system will be multi-swing stable. (More precisely, conditions (5.3) met after n swings do not guarantee $(n + 1)$-swing stability.) Hence, multi-swing stability should be investigated via further exploration of the multi-machine swing curves. Finally, eq. (5.4) is a mere approximate expression of a stable margin, since the angle δ_u is never reached but, rather, assessed approximately.
6. Computational requirements. The above SIME calculations (of the OMIB parameters and resulting transient stability information about critical machines and margins) require virtually negligible computing time (generally, much smaller than 5 % of the required T-D simulations).
7. The shape of an OMIB curve may differ significantly from the shape of an actual machine's swing curve. Indeed, the OMIB equivalent does not describe the behavior of an actual machine but, rather, the compressed information about the multi-machine system dynamics.
8. The identification of the group of critical machines is an issue of utmost importance. In some cases, the critical groups can be clearly identified during the whole simulation time. This has caused many researchers to try applying SIME in an incorrect way, in which they run the simulation first, until detecting instability by means of another criterion, like the maximum angular deviation, and then they identify the critical group as it can be observed at the end of the simulation.

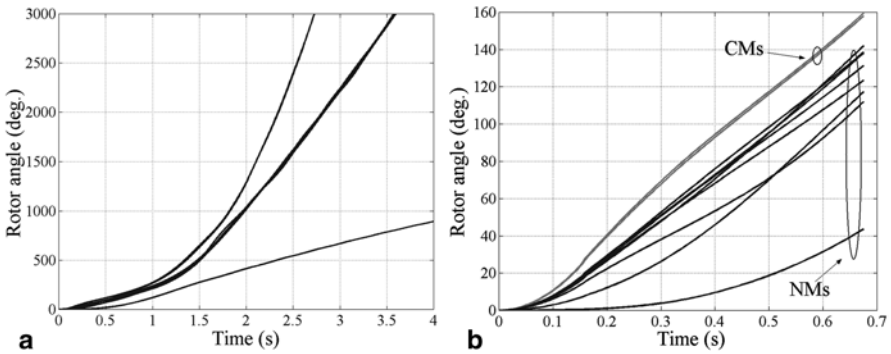

Fig. 5.6 Comparison of the groups of machines at the end of the simulation, and at the time instability conditions are met. **a** Multi-machine swing curves. **b** Identification of the CMs. (Adapted from Ruiz-Vega 2002)

Unfortunately, this procedure is not correct, since the actual critical group cannot always be easily observed at the end of the simulation as shown in *Fig.* 5.6. This case is also interesting because, as can be observed in *Fig.* 5.6a, it shows that the system machines are divided into three groups. Using SIME at each step of the T-D simulation, it is shown in *Fig.* 5.6b that the system machines are initially split into two groups, and that the instability conditions are met at a very early time of the simulation in which the group of machines when the simulation statistics is different from the one at the end of the simulation. This difference in machine groups makes it necessary to apply SIME at each time step of the simulation in order to correctly identify the group of critical machines.

5.2.4 Transient Oscillations Damping

5.2.4.1 Preliminaries

Today, online transient oscillations damping is becoming an issue of great concern, with the trend to include damping techniques as part of a transient stability function. An interesting online damping assessment technique uses the Prony method, where single- or multi-channel algorithms analyze one or several (up to, say, 15) generator swing curves at a time (Ruiz-Vega 2002; Ruiz-Vega et al. 2004). However, the quality of the analysis depends strongly on the number and proper identification of the relevant generator curves, whereas, generally, their number may exceed the algorithmic possibilities, and their identification may be far from obvious.

This may create serious difficulties when dealing with real-world power systems. SIME allows one to circumvent these difficulties by applying single-channel Prony analysis to the OMIB curve. Besides, by identifying the system machines that have a major influence on the oscillatory phenomena, it easily determines the

dominant modes of oscillation. Last but not least, it provides control techniques, able to improve transient oscillations damping as is described in Sect. 5.3.

5.2.4.2 SIME-Based Prony Analysis

For a given contingency, the SIME-based Prony analysis proceeds in the following way:

1. Run SIME to compute the transient stability limit (critical clearing time or power limit), using one stable and one or two unstable cases. The computation of such a limit relies on pair-wise extrapolation (or interpolation) of stability margins (§§ 5.3.2.3 and 5.3.5).
2. On the least unstable case, identify the critical machines and corresponding OMIB. Also, determine the "relative relevance" of each one of the critical machines, defined as the product of its inertia with its angle (absolute or relative to a reference), assessed at time t_u.
3. On the stable OMIB curve corresponding to the stable case in step 1 of this procedure, perform Prony analysis to assess the damping ratio of the OMIB swing curve.

Remarks:

1. The method assesses damping of nearly unstable contingency scenarios, which, generally, are the most interesting ones.
2. The Prony method has to analyze signals close to linear, if a direct comparison with modal analysis is required. This is often the case at the end of the data window, rather than at its inception, where the amplitude of the transients may be large.
3. The use of OMIB improves the Prony accuracy, robustness, and overall performance. Indeed, this second-order dynamic equivalent contains the key dynamics of machines exchanging energy. Besides, unlike other approaches, the OMIB rotor angle inherently captures the nonlinear and nonstationary dynamics of the system and can be used to determine linear and nonlinear attributes of system oscillations. Also, because of its formulation, the OMIB signals are less likely to include other less relevant dynamics, and this greatly facilitates the analysis of the slow dynamics of interest associated with the critical inter-area modes.

5.2.4.3 Sample of Illustrations

Ruiz-Vega et al. (2004) report on simulations performed on two real-world power systems using detailed system models: the EPRI 627-machine (4112-bus, 6091-line) system and the EPRI 88-machine (434-bus, 2357-line) system (Ruiz-Vega 2002; Ruiz-Vega et al. 2004).

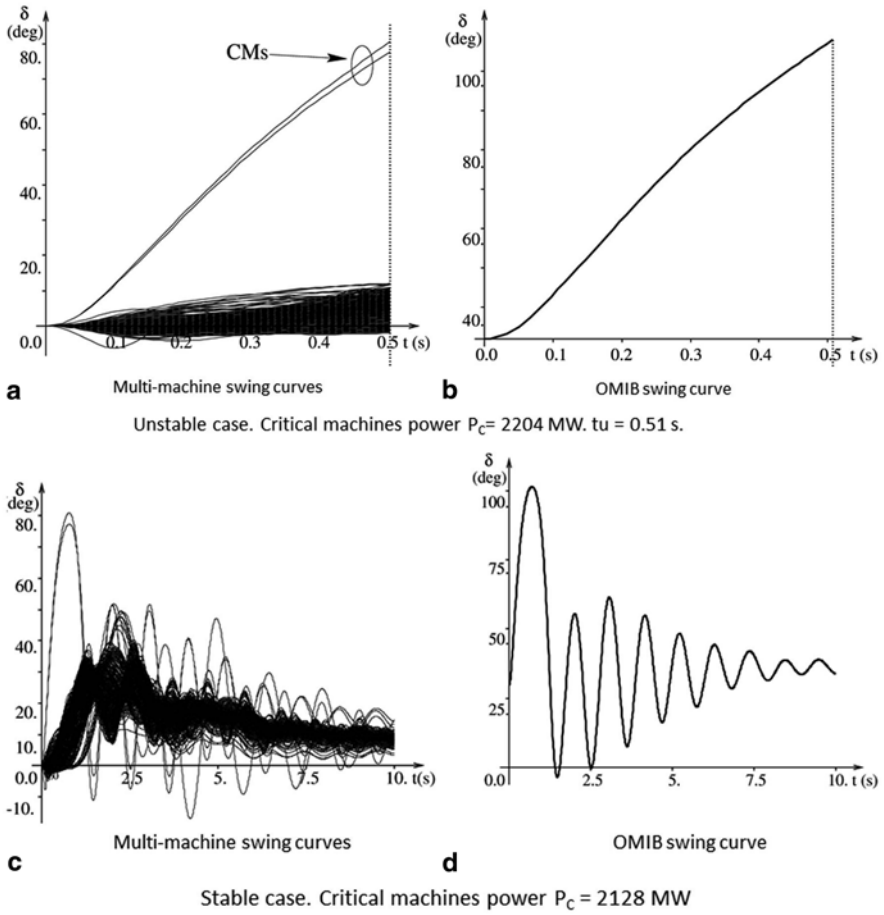

Fig. 5.7 Unstable and stable cases simulated on the EPRI 627-machine system. Unstable case: **a** Multi-machine swing curves, **b** OMIB swing curve; Stable case: **c** Multi-machine swing curves, **d** OMIB swing curve. Clearing time of both cases, 67 ms. (Adapted from Ruiz-Vega 2002)

The contingencies considered yield oscillatory plant modes (on the 627-machine system) and inter-area modes (on the 88-machine system). In all simulations, SIME is coupled with the ETMSP T-D program (EPRI 1994).

Plant Mode Oscillations

The plant-mode oscillations of the 627-machine system involve two critical machines. The resulting multi-machine swing curves of the considered post-fault stable case are displayed in Fig. 5.7c. The Prony analysis is applied to the OMIB swing curve of Fig. 5.7d, whose structure, as mentioned above, was defined on the unstable simulation displayed in Figs. 5.7a and 5.8.

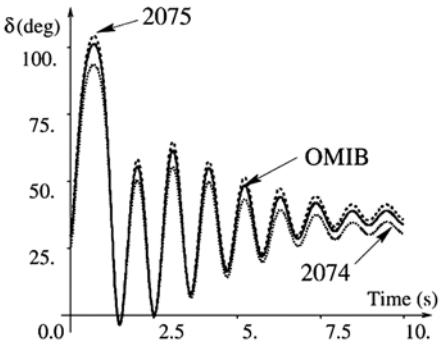

Fig. 5.8 Comparison of the swing curves of the OMIB and the critical machines (Nrs 2075 and 2074) of the stable case simulated on the EPRI 627-machine system. (Adapted from Ruiz-Vega 2002)

Table 5.1 Results of Prony analysis of the OMIB and the critical machine swing curves on the EPRI 627-machine system. (Adapted from Ruiz-Vega 2002)

α (rad/s)	ω (rad/s)	f (Hz)	ζ (%)	SNR (dB)
OMIB				
−0.483	5.84	0.930	8.23	42.35
Machine # 2075				
−0.509	5.83	0.927	8.7	43.27
Machine # 2074				
−0.474	5.83	0.928	8.0	35.89

Note that the two critical machines, defined on this unstable simulation, are easily identified also on the stable simulation. Hence, in this particular case, the choice of the generators to be analyzed is quite obvious; the SIME method and resulting OMIB are used here to illustrate the approach. Among various observations, we note the following:

1. In Ruiz-Vega et al. (2004), the original OMIB curve and the curve estimated by Prony have been displayed and shown to fit almost perfectly.
2. Also, Prony analysis has been performed on the two relevant machines identified by SIME (labeled #2075 and 2074). The result, displayed in *Fig.* 5.8, shows that the frequency of these two and of the OMIB curves is almost the same, while the value of the damping ratio of the OMIB lies in between that of machines 2075 and 2074. Table 5.1 gathers their damping features and shows that the numerical results are reflecting well the shapes and relative positions of the three curves.

Inter-Area Mode Oscillations

Application of a severe contingency to the EPRI 88-machine system has created an inter-area mode transient instability in which 36 machines lose synchronism with respect to the remaining 52 system machines. The swing curves of the unstable and stable cases are displayed in *Fig.* 5.9.

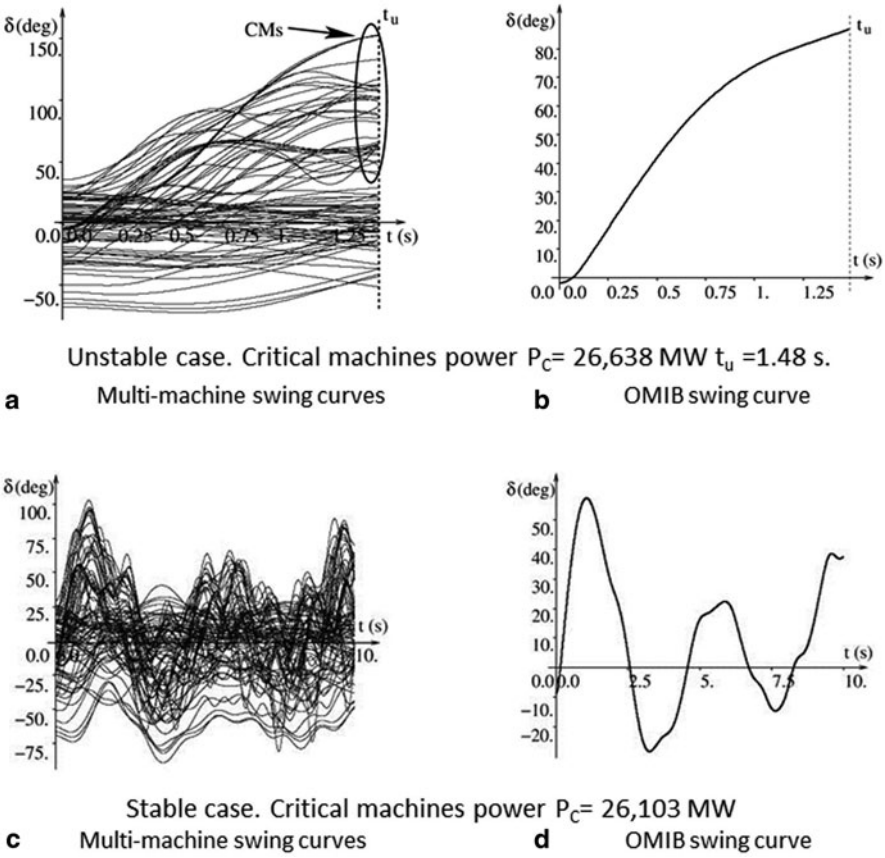

Fig. 5.9 Unstable and stable cases simulated on the EPRI 88-machine system. Unstable case: **a** Multi-machine swing curves, **b** OMIB swing curve; Stable case: **c** Multi-machine swing curves, **d** OMIB swing curve. Clearing time of both cases, 120 ms. (Adapted from Ruiz-Vega 2002)

Table 5.2 Damping assessment by Prony analysis of the OMIB swing curve for the EPRI 88-machine system. (Adapted from Ruiz-Vega 2002)

α (rad/s)	ω (rad/s)	*f* (Hz)	ζ (%)	SNR (dB)
−0.101	1.5117	0.24	6.6	42.29
0.206	5.5232	0.87	−3.7	

The Prony analysis performed on the stable case provides the results listed in Table 5.2. This table reveals that, actually, there are two dominant modes, and that for the above presumably "stable" case the damping ratio of one of them is negative, which suggests the existence of an unstable oscillation and predicts future system loss of synchronism. Actually, Ruiz-Vega et al. (2004) explain why the T-D simulation did not detect instability, by showing that this instability arises at 11.4 s,

i.e., beyond the preassigned maximum integration period of the simulation (10 s). Further, this reference suggests interesting by-products of this "early instability detection."

Again, the original OMIB curve and the curve estimated by Prony are shown to fit perfectly (Ruiz-Vega et al. 2004).

5.3 SIME-Based Transient Stability Control Techniques

Various SIME-based control techniques have recently been proposed (Zhang et al. 1997; Pavella et al., 2000a; Ruiz-Vega and Pavella 2003). This section describes three such techniques dealing with preventive control, closed-loop emergency control, and Open-Loop Emergency Control (OLEC); this latter aims at mitigating control actions taken preventively with emergency actions triggered only upon actual occurrence of the threatening event. All three techniques rely on the same principle, described hereafter.

5.3.1 Principle

To stabilize a case, SIME uses the size of instability (margin), the critical machines, and suggestions for stabilization. These suggestions are obtained by the interplay between OMIB–EAC and T-D multi-machine representations as follows: Stabilizing a case consists of modifying the pre- or post-contingency conditions until the stability margin becomes zero. According to EAC, this implies increasing the decelerating area and/or decreasing the accelerating area of the OMIB δ–P representation. In turn, this may be achieved by decreasing the OMIB equivalent generation power. The amount of the OMIB generation decrease required to stabilize the system, ΔP_{OMIB}, is directly related to the margin η (Pavella et al. 2000a; Ruiz-Vega et al. 2003):

$$\eta = f(\Delta P_{OMIB}). \tag{5.5}$$

5.3.2 Preventive Control (P-SIME)

5.3.2.1 Iterative Stabilization Procedure

It is shown that to keep the total consumption constant, the following multi-machine condition must be satisfied, when neglecting losses:

$$\Delta P_{\mathrm{OMIB}} = \Delta P_{\mathrm{C}} = \sum_{i \in \mathrm{CMs}} \Delta P_{\mathrm{C}_i} = -\Delta P_{\mathrm{N}} = -\sum_{j \in \mathrm{NMs}} \Delta P_{\mathrm{N}_j}, \tag{5.6}$$

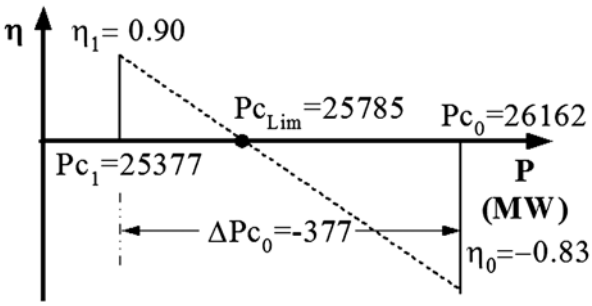

Fig. 5.10 Preventive SIME-based stabilization procedure of a relatively "mild" contingency. Conditions of Figs. 5.1 and 5.2. (Adapted from Ruiz-Vega 2002)

where ΔP_C and ΔP_N are the changes in the total power of the group of critical and noncritical machines, respectively.

Application of eqs. (5.5) and (5.6) provides a first approximate value of ΔP_C that may be refined via a stabilization procedure, which is iterative since the margin variation with stability conditions is not perfectly linear. Nevertheless, in practice, the number of required iterations (margins) seldom exceeds 3 (Pavella et al. 2000a; Ruiz-Vega et al. 2003).

5.3.2.2 Generation Rescheduling Patterns

Expression (5.6) suggests that there exist numerous patterns for distributing the total power change ΔP_N among noncritical machines, and whenever there are many critical machines, numerous patterns for distributing the total ΔP_C as well. The choice among various patterns may be dictated by various objectives, related to market or technical considerations.

In the absence of particular constraints or objectives, the total generation power could be distributed proportionally to the inertias of the noncritical machines. A more interesting solution consists of using an Optimal Power Flow (OPF) program, as discussed below, § 5.3.2.4. Finally, the above procedure may readily be adjusted for stabilizing several harmful contingencies simultaneously (Ruiz-Vega and Pavella 2003).

Remark: The above generation rescheduling procedure can also be used to enhance transient oscillations damping performance.

5.3.2.3 Illustrations

Below we apply the above P-SIME generation rescheduling to two stability scenarios: a relatively "mild" one and a severely stressed one.

Figure 5.10 sketches the simulations performed to stabilize the moderate instability described in *Figs.* 5.1 and 5.2, concerning a contingency applied to the EPRI 88-machine system and creating instability. More precisely, *Figs.* 5.1a and 5.2a describe the unstable case, *Figs.* 5.1b and 5.2b the stabilized case.

On the other hand, Table 5.3 describes the procedure for stabilizing the very severe contingency, which creates the severely stressed case displayed in *Fig.* 5.4.

Table 5.3 Preventive stabilization of a severe contingency. (Adapted from Ruiz-Vega 2002)

1	2	3	4	5	6
It.	η	Nr of	Pck	Pck + 1	sTDI
#	(rad/s)2	CMs	(MW)	(MW)	(s)
0	−12.52*	7	5600	5041	0.395
1	−9.70*	7	5041	3431	0.430
2	−1.66*	7	3431	2815	0.605
3	−2.898	7	2815	2731	0.935
4	−2.282	7	2731	2423	1.015
5	0.675	7	2423	2493	5.000

In column 6, sTDI stands for "seconds of time-domain integration." Recalling that computations of SIME per se are virtually negligible, sTDI is a handy measure of the time required by the T-D program to run a simulation; it therefore makes comparisons of computing performances independent of the computer, system size, and T-D program used

* The asterisk in column 2 indicates a surrogate margin

The asterisk in column 2 indicates a surrogate margin (see item 3 in § 5.2.3 and *Fig.* 5.4b).

Column 3 indicates that there are 7 critical machines out of the 88 system machines. In such a stressed case, the iterative procedure starts with surrogate margins until curves P_e and P_m intersect, then continues with standard margins. Note that, generally, very severe cases require a larger number of iterations.

Observe that the stabilization of this contingency imposes a generation decrease in the seven critical machines of over 50% of their total initial generation. This countermeasure might be deemed too expensive to apply preventively. The OLEC technique proposed in § 5.3.4 provides an interesting alternative (see the illustration of § 5.3.4.3).

5.3.2.4 Transient Stability-Constrained OPF

The OPF uses control variables like active and reactive generation powers to achieve a good tradeoff between security and economics. More specifically, this program optimizes the power system operating condition with respect to a prespecified objective (minimum operating cost, maximum power flow), while respecting generator limits and static security constraints (line power flows and bus voltage limits).

Several attempts have been made to imbed transient stability constraints within the OPF. According to the way of handling these constraints, they yielded two different approaches that below we call "global" and "sequential."

Global Approach A T-D simulation is run. The power system transient stability model is converted into an algebraic set of equations for each time step of this simulation. The set of nonlinear algebraic equations resulting from the whole T-D simulation is then included in the OPF as a stability constraint, forming a (generally huge) single nonlinear programming problem, e.g., see La Scala et al. (1998) and Gan et al. (2000).

Sequential Approach A T-D simulation is run. The transient stability constraints are directly converted into conventional constraints of a standard OPF program, e.g.,

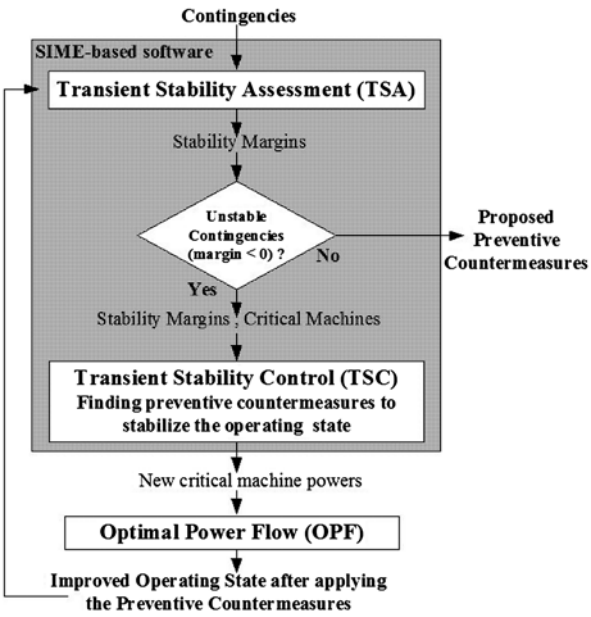

Fig. 5.11 Transient stability-constrained OPF (sequential approach). (Adapted from Ruiz-Vega 2002)

active generation power. Hence, they do not affect the size of the power system model and the complexity of the OPF solution method. They can use any conventional OPF program.

Figure 5.11 illustrates the use of the sequential approach, which, besides the above-mentioned advantages, may easily comply with market requirements thanks to the flexibility of choice among critical machines and noncritical ones on which generation can be re-dispatched.

The main drawback of the sequential approach is that it cannot guarantee optimality. Conceptually, the global approach is therefore more appealing: It is supposed to handle the problem as a whole and, hence, to provide an optimal solution, which would be accepted as the reference by the system operator and the electric market participants. However, its practical feasibility is questionable since it requires very heavy computations due to the huge nonlinear programming model.

5.3.2.5 Online Implementation of the sequential approach

Preventive TSA has been integrated into an online dynamic security assessment platform within the OMASES project funded by the European Commission (EU project OMASES—Open Market Access and Security Assessment System, EU Contract N. ENK6-CT2000-00064, December 2000). Three different operating modes are made available to system operators, i.e., engineering mode, real-time mode, and training mode (Cirio et al. 2005) as follows:

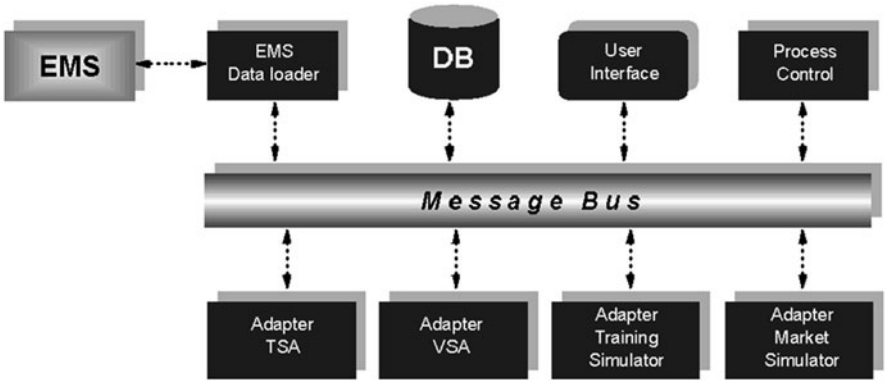

Fig. 5.12 OMASES architecture and application functions. (Taken from Cirio et al. 2005)

1. *Engineering mode:* off-line application of TSA and voltage stability assessment (VSA) studies involving or not the market environment and performed mainly for planning purposes.
2. *Real-time mode:* The Energy Management System (EMS) feeds OMASES with network data and solutions. DSA is synchronized with data transfer and cyclically runs with an overall execution time within 15 min.
3. *Training mode:* The operator gets used with the power system dynamics and DSA tools, and performs analysis (future scenarios, post-event analysis, etc.) of the existing electrical system and/or experiments. Market rules can be used to provide realistic scenarios.

Figure 5.12 depicts the OMASES platform. The EMS data loader transfers the state-estimator online snapshots to a relational database management system, from which the different functions (TSA, VSA, operator training, and market simulators) can access the data.

These latter functions are controlled by the process control module, which launches requests for analyses. The results are then sent back to the user interface via HTML files.

The TSA module of the OMASES platform is based on SIME coupled with the Eurostag T-D simulation software (Bihain et al. 2003). It is composed of a contingency filtering, ranking, and assessment module (called FILTRA (Ruiz-Vega et al. 2001)) and a preventive control module used for generation rescheduling, as described in Sect. 5.3.2.2. A typical screenshot of the FILTRA module's outputs is shown in Fig. 5.13.

Within the OMASES project, the TSA module based on SIME was tested on two real-world systems, namely the Greek extra high voltage (EHV) system (operated by Hellenic Transmission System Operator, HTSO) and the Italian EHV system (operated by Gestore della Rete di Trasmissione Nazionale, GRTN).

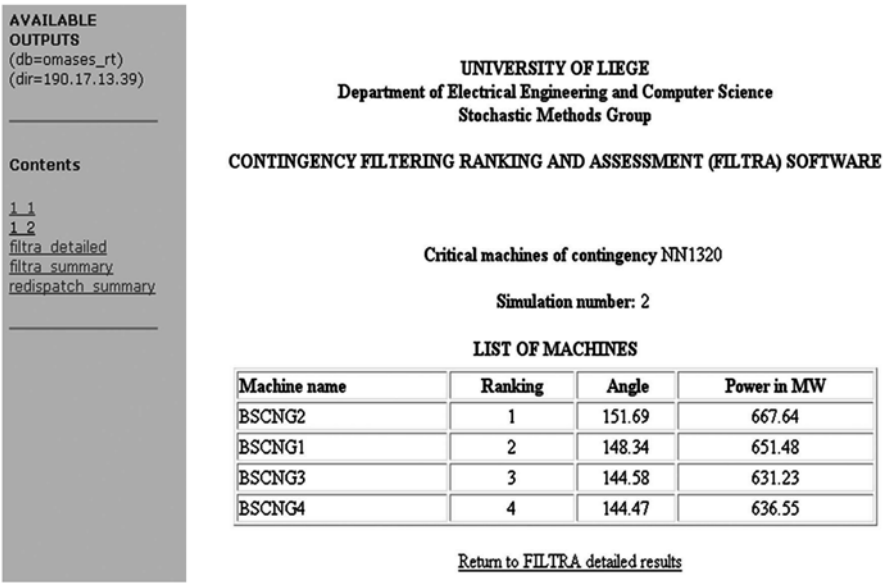

AVAILABLE OUTPUTS
(db=omases_rt)
(dir=190.17.13.39)

Contents

1_1
1_2
filtra_detailed
filtra_summary
redispatch_summary

UNIVERSITY OF LIEGE
Department of Electrical Engineering and Computer Science
Stochastic Methods Group

CONTINGENCY FILTERING RANKING AND ASSESSMENT (FILTRA) SOFTWARE

Critical machines of contingency NN1320

Simulation number: 2

LIST OF MACHINES

Machine name	Ranking	Angle	Power in MW
BSCNG2	1	151.69	667.64
BSCNG1	2	148.34	651.48
BSCNG3	3	144.58	631.23
BSCNG4	4	144.47	636.55

Return to FILTRA detailed results

Fig. 5.13 FILTRA results and critical machines of Brindisi power station. (Taken from Cirio et al. 2005)

5.3.2.6 Recent developments concerning the global approach

In recent investigations where SIME is applied to the global approach (Pizano-Martínez 2010; Pizano-Martínez et al. 2010, 2011), many of the drawbacks of this approach were solved, until arriving to a point where its practical feasibility has become a reality. We briefly describe the main ideas which led to this improvement.

Recall that the global approach originally uses two large sets of constraints, additional to the ones of a conventional OPF: the set of transient stability constraints (a set composed by a transient stability inequality constraint for each machine to keep its angle trajectory in a "stable regime") and the set of dynamic constraints (a typically very large set of nonlinear equality constraints resulting from the discretization of the power system dynamics, namely one subset of constraints for each time step of the considered integration period).

The first improvement proposed in Pizano-Martínez et al. (2010), and called below "Method 4," proceeds as follows:

1. For an unstable contingency, it first determines t_u and $\delta(t_u)$ of the relevant OMIB dynamics.
2. Next, by reducing the clearing time to the CCT, it determines the corresponding $\delta'(t_u)$ for this marginally stable case.
3. It then uses in the nonlinear program a single stability constraint, which imposes to change the operating point such that $\delta(t_u)$ becomes equal to $\delta'(t_u)$ (or slightly smaller).

4. The two above steps are iterated until the resulting operating point becomes indeed stable with respect to the initial contingency and given clearing time.

Notice that this approach already reduces the complexity of the nonlinear programming problem in a significant way, since it replaces the very large number of generator-wise stability constraints imposed over the whole integration period, by a single OMIB stability constraint imposed at a single time step t_u. Furthemore, since the full system dynamics need to be modeled only until t_u to express this stability constraint, this also reduces the number of dynamic constraints. Indeed, in practice, t_u is typically about one order of magnitude smaller than the whole integration period usually used in such transient stability studies.

The work presented in Pizano-Martínez et al. (2011) further builds on the previous ideas in order to reduce the dynamic constraints to the simplest possible expression. The rationale behind their method (called "New Approach," below) is the following:

1. The authors first notice that once the rotor angles and speeds of all generators are known at some time instant during the integration period, their subsequent dynamics are fully determined over the rest of the integration period (assuming a given fault scenario).
2. In particular, the dynamics thus only depend on the initial values of all rotor angles (since all initial speeds are all equal to zero).
3. Extrapolating this property to the dynamics of the relevant OMIB, they propose to express the stability constraint as an upper bound on the angle of this relevant OMIB at $t=0$. The whole nonlinear programming problem can therefore be formulated by using one single set of equality constraints at $t=0$, plus a single inequality constraint on the OMIB angle at $t=0$.

Building on these ideas, Pizano-Martínez et al. (2011) propose to iteratively force the initial OMIB angle progressively towards its marginally stable value (whose exact value is indeed not known beforehand). Schematically, this works in the following way:

1. For an unstable case, one first determines the relevant OMIB structure and computes its $\delta(t_0)$.
2. One then formulates and solves the nonlinear programming problem, so as to compute an operating point under the constraint that the initial angle becomes a bit (say 10 %) smaller than $\delta(t_0)$.
3. The two above steps are iterated until stability is reached, by exploiting linear extrapolation and linear interpolation as soon as a stable case is found (see Pizano-Martínez et al. 2011, for the details).

The resulting iterative approach turns out to be significantly faster than Method 4, while yielding the same level of accuracy (see below).

In order to have a general idea of the size reduction of the model achieved by this approach, if we denote N_b the number of buses of the system, N_s the number of integration time steps, and N_g the number of generators, the initial global approaches

Table 5.4 Comparison of **t**ransient **s**tability-**c**onstrained OPF **a**pproaches. (Adapted from Pizano-Martínez et al. (2011))

Total power generation cost ($/h)					
Base OPF	New approach	Method 1	Method 2	Method 3	Method 4
1132.18	1134.71	1191.56	1140.06	1134.01	1135.2

(Gan et al. 2000), using the classical model, require $N_g \times N_s$ additional stability constraints and $(2N_g + 2N_b) \times N_s$ additional dynamic constraints to solve the resulting OPF problem. For a small academic system with three generators and nine buses, considering simulations of 1 s with 0.01 time-step length, the number of additional constraints rises to 300 stability constraints and 2400 dynamic constraints, i.e., 2700 additional constraints. This number of additional constraints, as explained before, increases with system size. On the contrary, using the new approach with the SIME method, the number of additional constraints is the same for any system size and is limited to only one.

An additional advantage of applying SIME in the global approach to transient stability-constrained OPF is that the optimization process is driven by the sensitivity analysis of SIME margins, which makes it possible to reach the exact stability boundary by means of inter-extrapolations and avoid unnecessary T-D simulations, making this approach more efficient in finding a good compromise between economy and security, as discussed below (Pizano-Martínez et al. 2011).

After these important improvements, it was necessary to check if the reduction in the size of the optimization model had not caused a decrease in its performance. Some tests were made comparing the new global approach with other transient stability-constrained OPF approaches, in Pizano-Martínez et al. (2011). The results shown in Table 5.4 highlight that the new global approach, while strongly reducing the size of the nonlinear programming problem, maintains its accuracy in obtaining economic solutions.

The transient stability-constrained OPF methods that are compared in Table 5.4 can be described as follows: Method 1 (Nguyen and Pai 2003) uses a conventional OPF with a generation rescheduling based on a trajectory sensitivity method; Method 2 (Cai et al. 2008) uses a differential evolution global search algorithm, while Method 3 (Zárate-Miñano et al. 2010) and Method 4 (Pizano-Martínez et al. 2010) use the transient stability index based on an OMIB rotor angle to only reduce the number of stability constraints.

As expected, the most economic operating cost is achieved by the conventional OPF (i.e., without any stability constraints). It is important to notice that the approaches that use the SIME method (the new approach and Methods 3 and 4) calculate a similar generation cost. After analyzing the results, it was observed that Methods 1 and 2 had a more expensive final operating condition because they overstabilized the system. This happens because the optimization procedure in both methods is not directly taking into account the real stability boundary, while it is taken into account in all the SIME-based methods. However, regarding the size of the power system model for the optimization process, the new approach, while

reaching the same results as the other SIME-based approaches, only requires adding one single constraint to the conventional OPF model (Pizano-Martínez et al. 2011). Further work is required in order to extend these ideas to the simultaneous treatment of several contingencies.

5.3.3 Closed-Loop Emergency Control

Closed-loop emergency control relies on the "Emergency SIME" method. In short, E-SIME starts acting after a disturbance inception and its clearance. It aims at *predicting* the system transient stability behavior and, if necessary, at deciding and triggering control actions early enough to prevent the loss of synchronism. Further, it aims at continuously monitoring the system in a closed-loop fashion, in order to assess whether the control actions have been sufficient or should be reinforced.

The principle of the control technique remains the same with the preventive SIME, but its application has the following important differences (Zhang et al. 1997; Ernst et al. 1998; Ernst and Pavella 2000; Pavella et al. 2000a):

- The information about the multi-machine system is provided by real-time measurements rather than T-D simulations.
- The generation shift from critical machines is made here by shedding generation that is not compensated by a generation increase on noncritical machines (at least at the very first instants following the control action).
- The system status (unstable margin and critical machines) is *predicted rather than assessed* along the system transient trajectory.
- The resulting practical procedure is summarized below.

5.3.3.1 Predictive Transient Stability Assessment

The prediction relies on real-time measurements, acquired at regular time steps, t_i. The procedure consists of the following steps:

1. *Predicting the OMIB structure:* Use a Taylor series expansion to predict (say, 100 ms ahead) the individual machines' rotor angles; rank the machines according to their angles, identify the largest angular distance between two successive machines, and declare those above this distance to be the "candidate critical machines," the remaining ones being the "candidate noncritical machines." The suitable aggregation of these machines provides the "candidate OMIB."
2. *Predicting the* $P_a - \delta$ *curve:* Compute the parameters of this "candidate OMIB," and in particular its accelerating power and rotor angle, P_a and δ, using three successive data sets acquired for the three different times.
3. *Predicting instability:* Determine whether the OMIB reaches the unstable conditions (1).

If not, repeat steps (a) to (c) using new measurement sets.

If yes, the candidate OMIB is the critical one, for which the method computes successively the unstable angle δ_u, the corresponding time to instability, t_u, and the unstable margin expressed by (2).

4. *Validity test:* Observing that under given stability conditions *the* value of the (negative) margin should be constant, whatever the time step, provides a handy validity test: It consists of pursuing the above computations until reaching an (almost) constant margin value.

5.3.3.2 Salient Features

The method uses real-time measurements acquired at regular time intervals and aims at controlling the system in less than, say, 500 ms after the contingency inception and its clearance. The prediction phase starts after detecting an anomaly (contingency occurrence) and its clearance by means of protective relays. Note that this prediction does not imply identification of the contingency (location, type, etc.). The prediction is possible thanks to the use of the OMIB transformation; predicting the behavior (accelerating power) of all of the system machines would have led to totally unreliable results. There may be a tradeoff between the above-mentioned validation test and time to instability: The shorter this time, the earlier the corrective action should be taken, possibly before complete convergence of the validation test.

5.3.3.3 Structure of the Emergency Control Scheme

On the basis of real-time measurements taken at the power plants, the method pursues the following main objectives:

- To assess whether the system is stable or it is driven to instability; in the latter case,
- To assess "how much" unstable the system is going to be; accordingly,
- To assess "where" and "how much corrective action" to take (pre-assigned type of corrective action); and
- to continue assessing whether the executed corrective action has been sufficient or whether to proceed further.

Block 2 in Fig. 5.14 covers the two first steps: prediction of instability and its size, and of critical machines. Block 3 handles the control actions and determines the number of units to shed. Note that after the order of triggering the action has been sent, the method continues monitoring and controlling the system in a closed-loop fashion, until reaching stabilization.

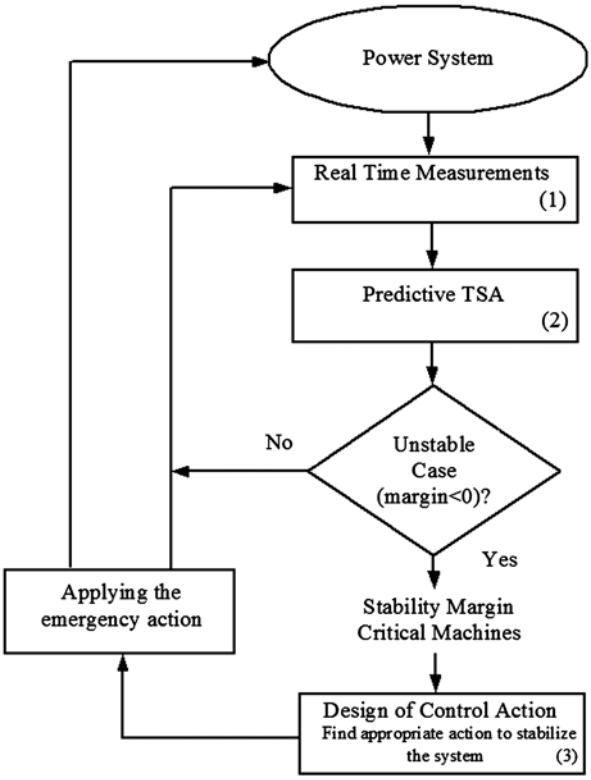

Fig. 5.14 Closed-loop transient stability emergency control: general framework. (Taken from Pavella et al. 2000)

5.3.3.4 Real-Time Implementation Concerns

The prediction of the time to (reach) instability may influence the control decision (size of control, time to trigger it, etc.).

The hardware requirements of the emergency control scheme are phasor measurement devices placed at the main power plant stations and communication systems to transmit (centralize–decentralize) this information. Already a few years ago, these requirements seemed to be within reach of technology (Phadke 1995).

The emergency control relies on purely real-time measurements (actually a relatively small number of measurements). This frees the control from uncertainties about power system modeling, parameter values, operating condition, and type and location of the contingency.

Within the EXaMINE project funded by the European Commission (IST 2000 26116), the actual implementation of E-SIME was examined from the viewpoint of designing a real-time measurement and communication system able to cope with the very stringent response-time constraints (Diu and Wehenkel 2002).

In particular, the question of real-time estimation and prediction of rotor angles from synchronized phasor measurements was investigated within the project, e.g., Del Angel et al. (2003).

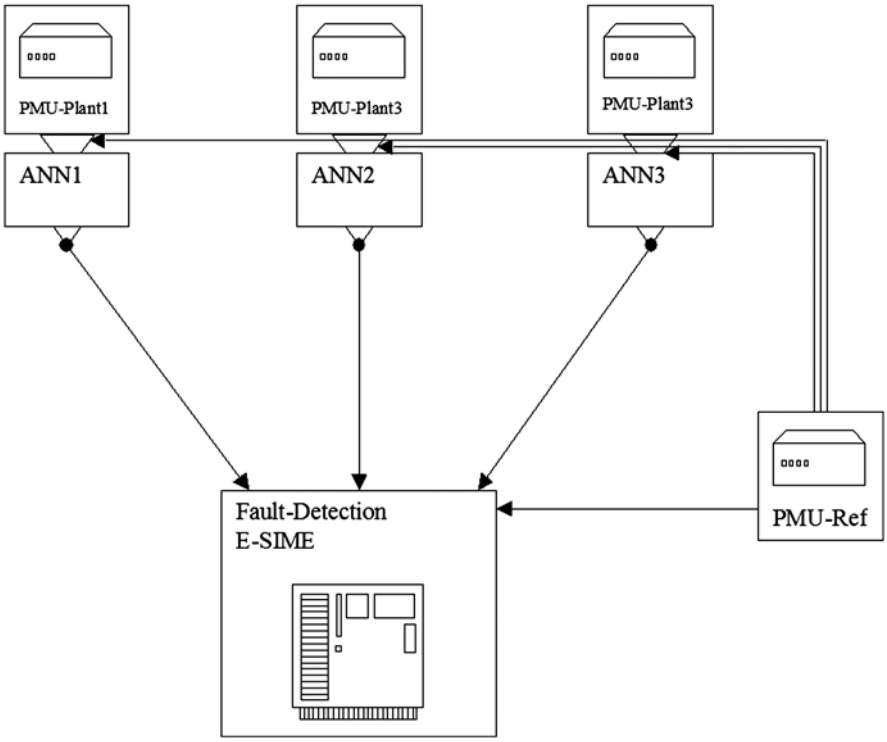

Fig. 5.15 Distributed rotor angle estimation and procedure using one PMU device and one artificial neural network per monitored power plant and one reference PMU

Figure 5.15 shows one of two possible schemes for the E-SIME implementation. This configuration encompasses two types of modules:

- *Distributed Artificial Neural Network (ANN)-based rotor angle estimation and prediction:* Each monitored power plant is equipped with a PMU device measuring the EHV side current and voltage phasors, at a rate of one per each 50-ms interval with respect to a common reference frame synchronized with the nominal frequency. These signals are then put into the actual system frequency reference frame by subtracting the phase signal obtained from a remote system bus (PMU-ref) and fed into the ANN module (three successive values) whose output furnishes an estimate of the current value of the power plant's average rotor angle and its predicted value two time steps ahead (100 ms). The ANN module is trained off-line using a detailed system and PMU model to generate input and output samples.
- *Central monitoring of loss of synchronism and emergency control:* This module receives the estimated and predicted values of rotor angles computed by the devices of the monitored plant, together with the voltage magnitudes of the PMU devices. These signals are monitored in order to detect fault occurrence near one

of the power plants and its clearing. Upon fault clearing, the E-SIME module is armed and starts monitoring the system dynamic behavior. As soon as loss of synchronism is predicted, the tripping signal is computed and sent to the critical power plant. The overall round-trip delay was estimated to be about 300 ms, which led to the conclusion of the feasibility of the E-SIME-based emergency control scheme.

The other implementation scheme that was examined in the EXaMINE project used a centralized version of the rotor angle estimation modules. With respect to the scheme of Fig. 5.15, this latter scheme has higher throughput requirements on the links from the monitored power plants to the central location, but reduces the number of channels from the PMU-Ref location (since this signal does not need to be broadcasted anymore to the individual plant locations).

Note that in both schemes it would be appropriate to introduce redundancy on the different devices and in particular in the common PMU-Ref device. The EXaMINE project led to the installation of six PMU devices on the Italian EHV system.

5.3.4 Open-Loop Emergency Control

5.3.4.1 Principle

This technique is a mixture of the preceding two techniques: From a methodological viewpoint, it is event driven and relies on transient stability simulations, like the preventive control technique, described in § 5.3.2; but its application uses generation tripping, like the emergency control technique, in addition to generation shifting.

The leading idea is to mitigate preventive actions (generation shifting) by complementing them with emergency actions (generation tripping) that would automatically be triggered only if the postulated contingency actually occurs. The technique relies on the assumption that (some of) the critical machines belong to a power plant equipped with a generation tripping scheme; therefore, a certain number of units could be tripped in the emergency mode.

Below, we outline the OLEC procedure in seven steps (Ruiz-Vega 2002; Ruiz-Vega and Pavella 2003).

5.3.4.2 Procedure

1. For an initially unstable scenario (operating condition subject to a predefined harmful contingency and its clearing scheme), compute the corresponding (negative) margin and determine the corresponding critical machines.
2. Assuming that (some of) these machines belong to a power plant equipped with a generation tripping scheme, select the number of units to trip in the emergency mode.

3. Run SIME, starting with the initial scenario up to reaching the assumed delay of generation tripping; at this time, shed the machines selected in step 2, and pursue the simulation until reaching instability or stability conditions (see eq. (5.1) and (5.3)). If stability is met, stop; otherwise, determine the new stability margin and corresponding critical machines (they might have changed from the previous simulation).
4. Run the transient stability control program (see § 5.3.2) to increase to zero this new (negative) margin. To this end, perform generation shifting in the usual way, from the remaining critical machines to noncritical machines. While performing this task, an additional objective may also be pursued, if the OPF software is combined with the transient stability control program.
5. The new, secure operating state results from the combination of the above generation rescheduling taken preventively and the consideration of the critical machines, previously chosen to trip correctively.
6. If there are more than one pattern of critical machines to trip, repeat steps 1–5 with each one of them, until getting an operating condition as close as possible to what is considered to be the "optimum" one (Ruiz-Vega and Pavella 2003).
7. After the number of machines to trip is determined, the settings of the special protection activating the generation tripping scheme in the plant is adapted so as to automatically disconnect these machines in the event of the contingency occurrence.

5.3.4.3 Illustration

Consider again the severe contingency that has been stabilized in the preventive mode in § 5.3.2.3. Recall that the corresponding stability case has seven critical machines, belonging to the same power plant, and having a total generation of 5600 MW in the transient stability-unconstrained pre-fault operating condition (Ruiz-Vega et al. 2003). Recall also that stabilizing this contingency in the purely preventive mode requires decreasing this generation to 2423 MW (see Table 5.1). Below, we consider again this contingency and stabilize it by OLEC, using the following parameters:

- Number of critical machines to trip: two; their stability-unconstrained pre-fault generation is $5600-4010=1590$ MW (see columns 4 of Tables 5.3 and 5.5).
- Time delay for tripping these critical machines: 150 ms.

Accordingly, the OLEC preventive generation rescheduling concerns the remaining five critical machines, whose stability-unconstrained pre-fault generation is 4010 MW.

The design of the control action follows the procedure of § 5.3.4.2. First, it is found that, because the case is very unstable, tripping two critical machines 150 ms after the fault inception would not be sufficient to stabilize it. Figure 5.16 describes the dynamics of the stability case, respectively before (Fig. 5.16a, b) and after tripping the two critical machines (Fig. 5.16c, d).

Table 5.5 OLEC stabilization of a very severe contingency (two machines tripped). (Adapted from Ruiz-Vega 2002)

1	2	3	4	5	6
It. #	η (rad/s)^2 (or MW)	Nr of CMs	Pc_k (MW)	Pc_{k+1} (MW)	sTDI (s)
0	−7.83*	5	4010	3609	0.421
1	−4.83*	5	3609	3260	0.461
2	−2.35*	5	3260	2662	0.506
3	−1.964	5	2662	2583	0.771
4	−1.265	5	2583	2440	0.856
5	−0.086	5	2440	2430	1.146
6	−0.036	5	2430	2415	1.216
7	0.028	5	2415	2422	5.000

* The asterisk in column 2 indicates a surrogate margin

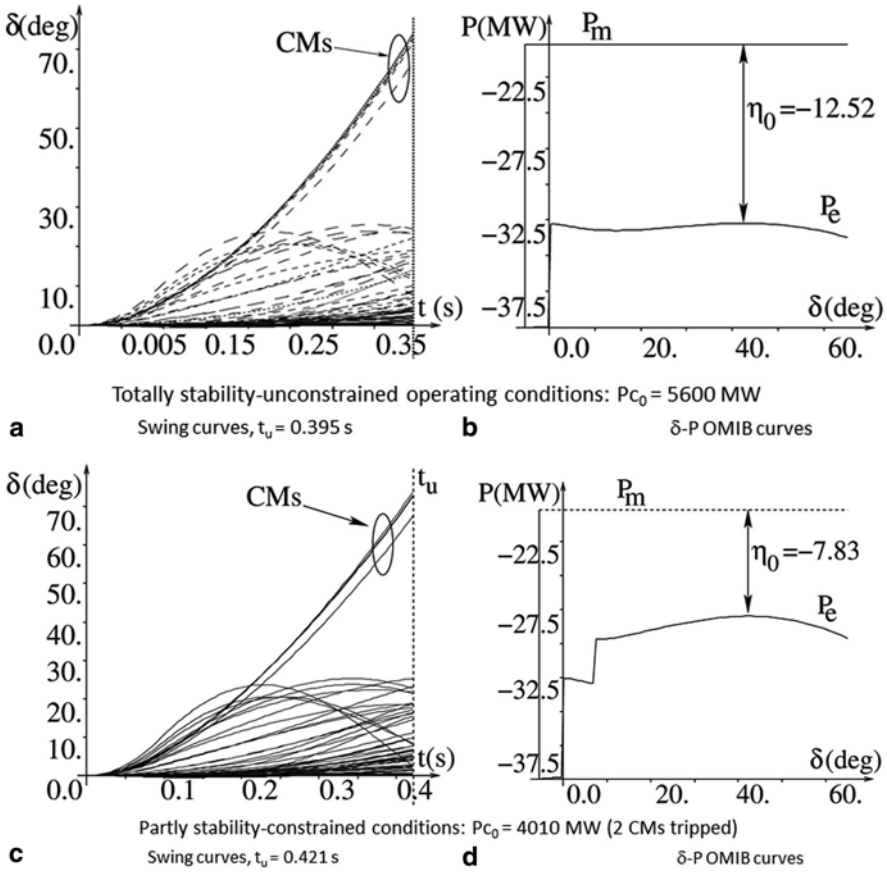

Fig. 5.16 Multi-machine swing curves and δ–P OMIB curves of two unstable cases. Totally stability-unconstrained operating conditions: **a** Swing curves, **b** δ-P OMIB curves; Partly stability-constrained conditions: **c** Swing curves, **d** δ-P OMIB curves. (Adapted from Ruiz-Vega 2002)

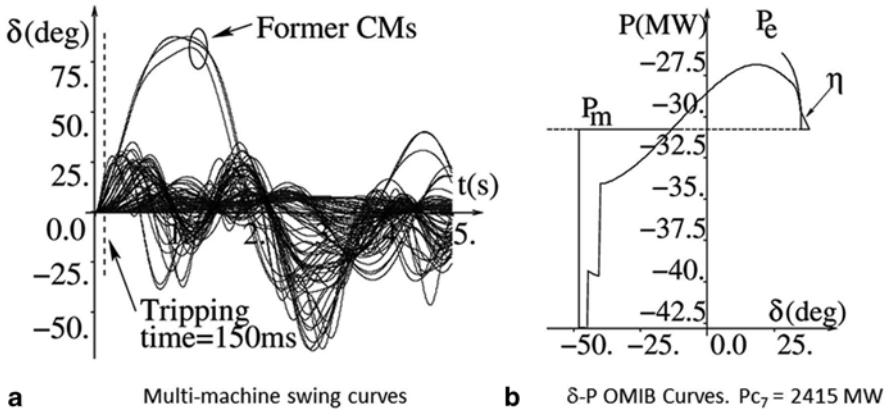

Fig. 5.17 Multi-machine swing curves and δ–***P*** OMIB curves of the stabilized case. Two generators are automatically tripped if the contingency actually occurs. (Adapted from Ruiz-Vega 2002)

More precisely, Figs. 5.16a, b portray, respectively, the multi-machine swing curves and the δ–P OMIB curves of the totally stability-unconstrained system.

Fig. 5.16c, d portray the curves corresponding to the partly controlled case, obtained by tripping two critical machines 150 ms after the contingency inception.

Comparing Fig. 5.16a, c suggests that the partly stability-constrained system is hardly less unstable than the unconstrained one: Compare the slope of their swing curves as well as their times to instability (395 ms vs. 421 ms). Similarly, comparing Fig. 5.16b, d shows that after the generation tripping (corresponding to $\delta_t = 7.34°$) the OMIB P_e curve gets somewhat closer to the P_m one, without, however, crossing it (their minimum "distance" decreases from 12.52 to 7.83 MW).

Since the emergency action is insufficient to stabilize the case, the procedure of § 5.3.4.2 continues with step 3: The new surrogate margin is computed and the appropriate preventive generation rescheduling is decided in order to stabilize the operating conditions.

The iterative procedure of rescheduling the five remaining machines is described in Table 5.5. The asterisk in column 2 indicates minimum distances between P_e and P_m OMIB curves, in MW, whereas "standard" margins are expressed in $(\text{rad/s})^2$.

See, for example, in row 0 of Table 5.5 and in Fig. 5.16d the margin of −7.83 MW. Row 7, column 4 of Table 5.5 provides the final result of the preventive stabilization procedure of the system with five critical machines; it indicates that their generation should be reduced to 2415 MW.

Figure 5.17 displays the multi-machine and OMIB δ–P curves corresponding to this stabilized case. They clearly show the effectiveness of the combined action of generation shifting (preventive) and generation tripping (emergency) controls. In particular, Fig. 5.17b shows that the OMIB equivalent power decreases from its initial value (−20.1 MW, see Fig. 5.16d) to its secure value (−30.7 MW), creating a decelerating area and making the system able to dissipate the kinetic energy gained by the five critical machines in the during-fault period.

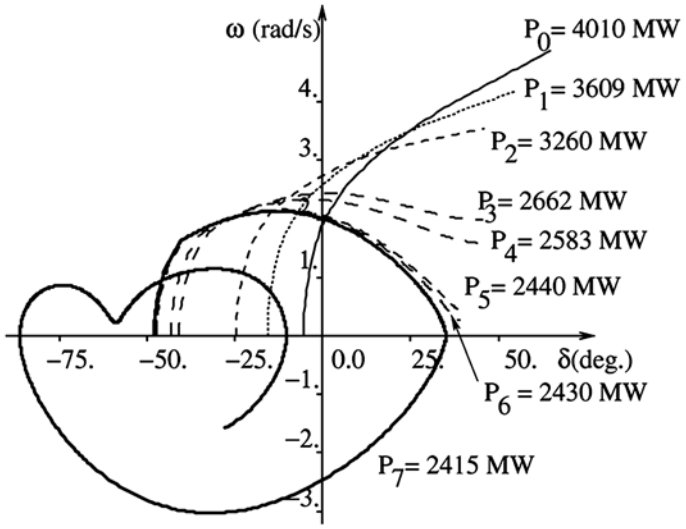

Fig. 5.18 OMIB phase plane representation of the seven simulations described in Table 5.5. Two generators tripped if the contingency actually occurs. (Adapted from Ruiz-Vega 2002)

A synopsis of the seven simulations listed in Table 5.5 is given in Fig. 5.18, plotting the OMIB phase plane. Incidentally, observe how clearly this plot describes the system dynamics under the various conditions.

In summary, to stabilize the considered severe contingency by OLEC, one should decrease preventively the pre-fault generation of the five critical machines (CMs) from 4010 to 2415 MW, under the assumption that the other two CMs would be tripped correctively, after the contingency inception.

Once the conditions of the stabilization process are obtained, the special protection activating the generation tripping in the plant is armed to *automatically* disconnect the selected plants in case the contingency *actually occurs*. The remaining five machines are rescheduled to their new values.

The pre-fault power of the plant, however, has been improved, with respect to the results presented in Table 5.3 (2415 + 1590 = 4005 MW by OLEC vs. 2423 MW by P-SIME in purely preventive mode).

5.3.5 Limit Search

Stability margins computed by SIME may be readily exploited to accelerate the computation of transient stability-constrained power flow limits and TTC/ATC calculations. Typically, the calculation of a power flow limit by dichotomy search requires about eight to ten runs (each run is composed of a power flow calculation and a T-D simulation for each contingency). By exploiting the stability margins one can

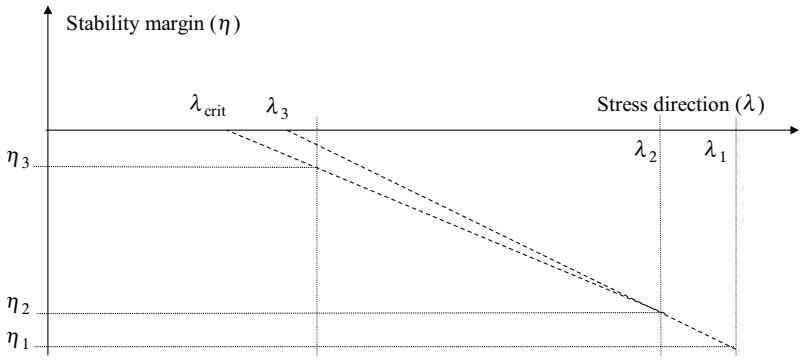

Fig. 5.19 Acceleration of limit search by SIME

use extrapolation or interpolation in order to reduce this number to three (Pavella et al. 2000b; Ruiz-Vega et al. 2002).

Figure 5.19 illustrates this idea graphically. The first simulation corresponds to the upper bound of the search interval (λ_1, the most stressed base case, for the given stress direction, yielding the margin η_1), The second simulation corresponds to a 10 % reduction of the stress parameter, leading in the illustrated case to a second unstable simulation (λ_2, η_2).

The two unstable margins are then exploited to estimate by linear extrapolation the critical value of the stress parameter. If this value is far from the second value (as depicted in Fig. 5.19), a third and last simulation is carried with a slightly higher value (λ_3 on Fig. 5.19) to improve accuracy. The final estimate of the critical value (λ_{crit}) is obtained from the two smaller, in absolute value, unstable margins.

5.4 Discussion

5.4.1 A Pragmatic Approach to Integrated Security Control

5.4.1.1 Preventive Mode Security Control

Preventive mode security assessment and control methods and software tools have been developed separately for static security, transient stability, and voltage stability. In principle, these tools are able to identify harmful contingencies and preventive control actions to alleviate insecurities from each point of view. However, each method concentrates only on part of the overall security control problem and hence its recommendations are generally not fully satisfactory from a global point of view.

It is thus necessary to incorporate these methods into a single decision support tool for secure online operation. Such a tool would ensure at the same time static

and dynamic security with respect to a list of potentially harmful contingencies identified during the analysis stage. We propose to use the optimal power flow formulation as a generic approach to handle this problem.

More specifically, let CL-SS be a list of potentially harmful contingencies from the viewpoint of static security, CL-TS a list of such contingencies from the viewpoint of transient stability, and CL-VS a list of potentially harmful contingencies from the viewpoint of voltage stability.

Then, we can formulate an optimization problem incorporating the following constraints:

1. *Operating (i.e., preventive mode) constraints:* pre-contingency power flow equations, and equality and inequality constraints (voltage magnitudes in normal range and branch flows below steady-state limit, operating limits, transactions, etc.).
2. *Static security constraints:* for each element in CL-SS a set of post-contingency power flow equations, and equality and inequality constraints (voltage magnitudes in emergency range and branch flows below emergency state limit).
3. *Transient stability constraints:* for each element in CL-TS a constraint on the total normal mode generation of the corresponding set of critical generators (note that such constraints can be derived by P-SIME).
4. *Voltage stability constraints:* for each element in CL-VS one (or several) constraints on the normal mode active and reactive power injections ensuring voltage stability with respect to that contingency (e.g., see Carpentier et al. 2001; Capitanescu and Van Cutsem 2002; and Bihain et al. 2003, for an approach yielding such information).

For a given objective function (e.g., minimal deviation, minimal cost of reschedule), the solution of such an optimization problem can be computed by a conventional security-constrained OPF. As long as the number of elements of CL-SS remains small, the CPU time required by a single run of such a tool remains compatible with online requirements.

Nevertheless, there is no guarantee that the resulting rescheduled operating point exists (feasibility) and is simultaneously secure with respect to all three security criteria. Thus, in principle, it would be necessary to iterate the above resolution scheme according to the same principle as the one given in *Fig.* 5.10.

Note also that there is no absolute guarantee that such an iterative process would converge in a reasonable number of iterations, and if yes, that the resulting new operating point would indeed be optimal. Nevertheless, we believe that such an integrated preventive security control framework is feasible and would be of value to online operation under stressed conditions.

We notice that the approach proposed relies on the availability of DSA tools able to express approximations to dynamic security regions in terms of pre-contingency parameters. The more accurate these approximations are, the better the resulting optimization will be. In particular, we believe that the proposed scheme is reasonable when combined with methods such as P-SIME and VSA.

5.4.1.2 Emergency Mode Security Control

While in preventive mode it is necessary to combine into a single coherent decision-making strategy the handling of all security constraints (because they may be conflicting), in emergency mode security control one can generally take advantage of the temporal decoupling of the different phenomena, since thermal problems are typically significantly slower than voltage collapses which in turn are typically much slower than loss of synchronism. Hence, the different emergency control schemes can operate independently from each other.

5.4.2 Limitations and Further Research Needs

5.4.2.1 Arbitration between Preventive and Emergency Control

A first limitation of the current security control approaches lies in the fact that they are not able to arbitrate between preventive and emergency control. More precisely, the current approach supposes that the contingencies and phenomena that must be treated in a preventive way are given a priori in the form of a list of "credible" contingencies and a set of static and dynamic constraints. Preventive security control then tries to change the operating conditions so that these constraints are satisfied for all contingencies. Emergency control is supposed to handle all other, non-credible, disturbances.

However, from a rational point of view the fact that a certain security problem (or constraint) should be treated in preventive or in emergency mode actually depends on operating conditions (electrical ones, economic ones, and meteorological ones as well).

For example, if a certain N-2 contingency becomes very likely (e.g., because of changing weather conditions), or if the cost of treating it in preventive mode is low (e.g., because there is cheap load curtailment available), then it could make sense to handle it in preventive mode, rather than in emergency mode.

Thus, in principle, the arbitration between preventive and emergency mode security control should be an output of (and not an input to) the security control decision support tools. However, there are intrinsic difficulties in achieving this objective mainly because of lack of data on probabilities of contingencies (as a function of real-time conditions) and difficulties to model the costs of interruptions, both of which would be required to allow a better coordination of preventive and emergency mode security control (Wehenkel 1999).

5.4.2.2 New Control Devices

New control devices such as variable series compensation, as well as more systematic use of interruptible load, can potentially make it easier to handle security

in online operation. However, the analytical methods developed today, like SIME, VSA, etc., do not take into account these possibilities. Thus, further adaptations are needed in order to develop tools able to suggest how to use such devices.

5.4.2.3 Uncertainties

A major problem in large-scale systems is that of real-time information concerning the status of neighbor systems and the incorporation of this information into appropriate dynamic equivalents needed to carry out meaningful simulations and DSA computations in real time.

The unavailability of this information translates into modeling uncertainties, which should be taken into account in a conservative way. Here also, research and developments are necessary in order to reduce the amount of arbitrariness of security control (Diu and Wehenkel 2002).

The addition of new generating plants based on renewable energies (wind and solar power plants mainly) have also increased the uncertainty in predicting the power system operating state, since their power output can change, in large amounts, in a very short period of time, due to faults or weather conditions. This is an additional difficulty to apply both preventive and emergency control.

5.4.2.4 Inter-Area and Inter-Temporal Coordination

In large power system interconnections, the security control of the overall system is presently organized in a distributed multi-area fashion. Each area is controlled by a system operator, responsible for the security in his/her area. One can show that bad coordination of these control agents can lead to quite suboptimal operation in each area of the system (Zima and Ernst 2005).

Also, the overall security of the system strongly relies on the quality of the exchange of information between different areas, in the form of static and dynamic equivalents as well as threatening disturbances.

To circumvent these difficulties, the trend has been in the USA to create MEGA System Operators responsible for the overall security, leading to the necessity to handle huge supervisory control and data acquisition (SCADA)/EMS databases and the explosion of computational requirements for security assessment and control software.

In other places and, particularly, in Europe, the trend has been to attempt to improve data exchange and coordination between the different existing system operators. In both cases, however, a sound-distributed security assessment and control approach, defining in a systematic and transparent way appropriate coordination schemes among areas, would be of great value.

In a similar fashion, a better coordination of security control decisions over different time horizons, i.e., operation planning, day ahead, real time, next hour, next day, etc., could help improve security and at the same time reduce costs. This would

lead to state security control as a sequential decision problem, which could be tackled in the framework of stochastic or dynamic programming (Wehenkel 2004).

5.4.2.5 Wide-Area Transient Stability Emergency Control

The networks of synchrophasors that are already installed in some countries can be used to develop a wide-area transient stability emergency control that monitors the system state in order to verify if the action of other preventive controls, and/or fast event-based emergency controls, has been able to stabilize the system. This system would act "in extremis," as a backup control, in case an additional control action would be required to stabilize the system.

This type of control is a new application of the emergency SIME method in the following aspects: It would not be applied to analyze a power plant but it would consider the stability of the whole power system; in addition, the critical machines could change along with the operating conditions and the actual fault. One advantage of this application of E-SIME is that it will have more time to act, since preventive control and the fast event-based controls had already been applied, giving, in this way, more time for applying the method in case the system would require an additional control action.

5.5 Conclusion

The present chapter has pursued a twofold objective. On the one hand, it has addressed the issue of real-time transient stability control, which has long been considered to be extremely problematic if at all feasible. Three different schemes have been advocated, able to encounter a variety of specific needs, depending on power systems specifics.

It was shown that preventive control and its variant, the OLEC, are mature enough and ready for implementation. Closed-loop emergency control, on the other hand, is very much dependent on today's high tech; its implementation requires strong incentives so as to foster the necessary investment in modernized communication infrastructure and monitoring equipment.

The second objective was an attempt towards integrated security control techniques, able to cover all dynamic and steady-state security aspects. It appeared that the software tools available today are able to achieve such integrated approaches.

Nevertheless, while from a theoretical viewpoint the above-advocated approaches are within reach, their realization depends on information about the system configuration, including generation status that the liberalized electricity markets seem reluctant to provide. And although such issues have not been addressed in this chapter, these authors feel that blackouts will continue threatening the power systems, unless such information is made available, under the pressure of regulatory bodies in the USA, Europe, and other continents.

Acknowledgments Prof. Mania Pavella contributed to the first version of this chapter (Wehenkel et al. 2005). The authors gratefully acknowledge her scientific work, encouragement, and support for developing this updated version.

References

Bihain A, Cirio D, Fiorina M, Lopez R, Lucarella D, Massucco S, Ruiz-Vega D, Vournas CD, Van Cutsem T, Wehenkel L (2003) Omases—a dynamic security assessment tool for the new market environment. In: Proceedings of IEEE Bologna power tech

Cai HR, Chung CY, Wong KP (2008) Application of differential evolution algorithm for transient stability constrained optimal power flow. IEEE Trans Power Syst 23(2):719–728

Capitanescu F, Van Cutsem T (2002) Preventive control of voltage security: a multi-contingency sensitivity-based approach. IEEE Trans Power Syst 17:358–364

Carpentier J et al (2001) Application of a new security concept in optimal power flows to congestion management. In: Proceedings of the 6th international workshop on electric power system control centers, Opio, France, June 10–13

Cirio D, Lucarella D, Vimercati G, Morini A, Massucco S, Silvestro F, Ernst D, Wehenkel L, Pavella M (2005) Application of an advanced transient stability assessment and control method to a realistic power system. To appear in Proceedings of PSCC05

Del Angel A, Glavic M, Wehenkel L (2003) Using artificial neural networks to estimate rotor angles and speeds from phasor measurement. In: Proceedings of intelligent systems applications to power systems, ISAP03

Diu A, Wehenkel L (2002) EXaMINE—experimentation of a monitoring and control system for managing vulnerabilities of the European infrastructure for electrical power exchange. In: Proceedings of IEEE PES summer meeting

EPRI (1994) Extended transient midterm stability program version 3.1 user's manual. Final Report EPRI TR-102004, Projects 1208-11-12-13

Ernst D, Pavella M (2000) Closed-loop transient stability emergency control. In: Proceedings of IEEE/PES winter meeting, Singapore

Ernst D, Bettiol A, Zhang Y, Wehenkel L, Pavella M (1998) Real time transient stability emergency control of the south-southeast Brazilian system. In: Proceedings of SEPOPE, Salvador, Brazil, (invited paper, IP044)

Gan D, Thomas RJ, Zimmerman RD (2000) Stability-constrained optimal power flow. IEEE Trans PWRS 15(2):535–540

La Scala M, Trovato M, Antonelli C (1998) On-line dynamic preventive control: an algorithm for transient security dispatch. IEEE Trans PWRS 13(2):601–610

Nguyen TB, Pai MA (2003) Dynamic security-constrained rescheduling of power systems using trajectory sensitivities. IEEE Trans Power Syst 18(2):848–854

Pavella M, Ernst D, Ruiz-Vega D (2000a) Transient stability of power systems: a unified approach to assessment and control. Kluwer, The Netherlands

Pavella M, Wehenkel L, Bettiol A, Ernst D (2000b) An approach to real-time transient stability assessment and control. Techniques for power system stability limits search—IEEE special publication no TP-138-0

Phadke AG (1995) Synchronized phasor measurements in power systems. IEEE Comput Appl Power 6(2):10–15

Pizano-Martínez A (2010) Determination of steady-state and transiently stable optimal equilibrium points in electric power systems. PhD Thesis, Universidad Michoacana de San Nicolás de Hidalgo, Morelia, Michoacán, México

Pizano-Martínez A, Fuerte-Esquivel CR, Ruiz-Vega D (2010) Global transient stability-constrained optimal power flow using an OMIB reference trajectory. IEEE Trans Power Syst 25(1):392–403

Pizano-Martínez A, Fuerte-Esquivel CR, Ruiz-Vega D (2011) A new practical approach to transient stability-constrained optimal power flow. IEEE Trans Power Syst 26(3):1686–1696

Ruiz-Vega D (2002) Dynamic security assessment and control: transient and small signal stability. PhD Thesis, University of Liège

Ruiz-Vega D, Pavella M (2003) A comprehensive approach to transient stability control. Part I: near optimal preventive control. Part II: open loop emergency control. IEEE Trans Power Syst 18(4):1446–1460

Ruiz-Vega D, Pavella M, Hirsch P, Sobajic D, Ernst D (2001) A unified approach to transient stability contingency filtering, ranking and assessment. IEEE Trans Power Syst 16(3):435–443

Ruiz-Vega D, Olguín Salinas D, Pavella M (2002) Simultaneous optimization of transient stability-constrained transfer limits of multi-area power systems. In: Proceedings of med power 2002 conference, Athens

Ruiz-Vega D, Messina A, Pavella M (2004) Online assessment and control of transient oscillation damping. IEEE Trans Power Syst 14(2):1038–1047

Wehenkel L (1999) Emergency control and its strategies. In: Proceedings of PSCC99, vol 1, pp 35–48, Trondheim

Wehenkel L (2004) Whither dynamic congestion management? Proceedings of bulk power system dynamics and control—VI, IREP04, 2 pages

Wehenkel L, Ruiz-Vega D, Ernst D, Pavella M (2005) Preventive and emergency control of power systems. In: Real time stability in power systems. Springer, Norwell

Zárate-Miñano R, Van Cutsem T, Milano F, Conejo AJ (2010) Securing transient stability using time-domain simulations within an optimal power flow. IEEE Trans Power Syst 25(1):243–253

Zhang Y, Wehenkel L, Pavella M (1997) A method for real-time transient stability emergency control. In: Proceedings of CPSPP97, IFAC/CIGRE symposium on control of power systems and power plants, Beijing, pp 673–678

Zima M, Ernst D (2005) On multi-area control of electric power systems, PSCC, Paper 2 in Session 9, Liege, Belgium, August 2005, Liège